

Anticancer Activity of New Organotin Complexes with Heterocyclic Thioamides

D. A. Berseneva^a, D. B. Shpakovsky^{a, *}, E. A. Nikitin^a, V. E. Goncharenko^{b, c}, Yu. A. Gracheva^a, K. A. Lyssenko^a, Yu. F. Oprunenko^a, and E. R. Milaeva^a

^a Moscow State University, Department of Chemistry, Moscow, Russia

^b Lebedev Physical Institute, Russian Academy of Sciences, Moscow, Russia

^c Higher School of Economics (National Research University), Moscow, Russia

*e-mail: dmshpak@mail.ru

Received April 5, 2023; revised May 2, 2023; accepted May 4, 2023

Abstract—New complexes **I**–**IV** of di-*tert*-butyltin with ligands based on heterocyclic thioamides (2-mercaptopbenzoxazole, 2-mercaptopbenzothiazole, 2-mercaptopbenzimidazole) and 2,6-di-*tert*-butyl-4-mercaptopphenol are synthesized and studied by X-ray diffraction (XRD). The XRD results for single crystals of **I**, **II**, and **IV** are presented (CIF files CCDC nos. 2251495, 2251493, and 2251494, respectively). Specific features of the synthesized crystal structures are discussed. Complexes **I** and **II** contain the expected Sn–C and Sn–S bonds and an additional coordination with the nitrogen atom in the heterocycles, which indicates the octahedral environment of the Sn(IV) atom (coordination number 6). The coordination polyhedron in complex **IV** can be described as a distorted tetrahedron (coordination number 4). The proposed compounds are studied as antiproliferative agents. Their antiproliferative activity is determined using the human cancer cell lines (PC3, MCF-7, HCT116, A549, and normal cells WI38). A dependence of the activity on the ligand structure is found. A comparative evaluation of the activity shows that the introduction of the antioxidant 2,6-di-*tert*-butyl-4-mercaptopphenol fragment into complex **IV** substantially decreases the cytotoxicity.

Keywords: organotin compounds, thiolates, crystal structure, thioamides, cytotoxicity

DOI: 10.1134/S1070328423600559

INTRODUCTION

Organotin compounds are characterized by a broad range of biological activity. The mechanisms of toxic effect of the organotin compounds are very diverse. The main factors of cell death are considered to be the interaction of the tin compounds with cell membranes, promotion of oxidative DNA damage, and apoptosis induction [1]. The structures with the Sn–C bond are resistant and have a high cytotoxic activity against cancer cells, which makes them promising candidates for the development of new anticancer drugs [2–4].

We have previously tested the series of the organotin complexes containing the 2,6-di-*tert*-butylphenol fragment on the human breast adenocarcinoma cells (MCF-7) and human cervical cancer cells (HeLa). The toxicity of the compounds was also evaluated toward the normal cells (human lung fibroblasts MRC-5). The range of IC₅₀ of the compounds varies from 0.16 to 30 μM for all tested cell lines. The highest activity toward both cell lines was determined for the triphenyltin complex based on 2,6-di-*tert*-butyl-4-mercaptopphenol with IC₅₀ equal to 250 nM (MCF-7) and 160 nM (HeLa), respectively. In addition, a sub-

stantial decrease in the toxicity of the complex toward the normal cells due to its protective antioxidant phenol fragment [5]. A significant antiproliferative activity of this compound is related, most likely, to its high lipophilicity and the ability to interact with the SH groups of tubulin protein as a possible target, to depolarize mitochondria, and to induce mitochondria swelling, which can also contribute to its cytotoxicity. Computer docking demonstrates a possibility of this molecule to interact with the colchicine site of tubulin [6].

Since the mechanism of action of the majority of anticancer organometallic compounds is based on the ligand exchange, a broad range of studies is aimed at varying the ligands bearing the O, N, and S donor atoms that provide the coordination with the Sn atom [7].

The purine fragment is a component of such important biomolecules as DNA, RNA, ATP, nicotinamide adenine dinucleotide (NAD) coenzyme, and others. BioisostERICALLY modified purine derivatives with diverse heterocyclic fragments were approved as anticancer drugs [8].

On the one hand, the chemotherapeutic agent nocodazole contains the benzimidazole core and inhibits (due to the tubulin-binding activity) assembling of tubulin microtubes [9]. On the other hand, we found the inhibitory effect on the polymerization of tubulin of the organotin complexes bearing the 2,6-di-*tert*-butylphenol fragments. The compounds showed a high cytotoxic activity exceeding that for cisplatin on the MCF 7 cancer cell line [6].

The antiproliferative activity is known for the organotin compounds bearing fragments of the following heterocyclic thioamides: 2-mercaptopbenzoxazole, 2-mercaptopbenzothiazole, and 5-chloro-2-mercaptopbenzothiazole. The studied complexes manifested a pronounced anticancer activity on the cancer cell line of leiomyosarcoma in rats. In addition, the complexes inhibited the activity of the lipoxygenase (LOX) enzyme, which is involved in the initiation of the cancer cell growth [10]. The antiproliferative activity of the complexes correlated with the inhibitory activity [11].

Thus, the N-, O-, and S-containing aromatic heterocycles are efficient complexing agents for the synthesis of modified organotin compounds. The differences in the ligand structure makes it possible to accomplish diverse coordination modes with the Sn(IV) atom, which can favor the modulation of biological activity.

In this work, we report the synthesis of dialkyltin bis(thiolates) based on heterocyclic thioamides and 2,6-di-*tert*-butyl-4-mercaptophenol and present the results of a comparative study of their antiproliferative activity and capability of inhibiting lipoxygenase enzyme.

EXPERIMENTAL

Tin(IV) thiolates were synthesized using commercially available bis(*tert*-butyl)tin dichloride (Sigma-Aldrich, 98%), 2-mercaptopbenzothiazole (Sigma-Aldrich, 97%), 2-mercaptopbenzoxazole (Sigma-Aldrich, 95%), and 2-mercaptopbenzimidazole (Sigma-Aldrich, 98%). 2,6-Di-*tert*-butyl-4-mercaptophenol was synthesized according to a known procedure [12]. Solvents were used as received.

¹H and ¹³C NMR spectra were recorded on a Bruker AMX-400 instrument in CDCl₃ or DMSO-d₆ (¹H, 400 MHz; ¹³C, 100 MHz; ¹¹⁹Sn 149 MHz). IR spectra were detected on an IR 200 FT-IR spectrophotometer (Thermo-Nikolet) in KBr pellets. Elemental analysis was conducted on a Vario Microcube analyzer (Elementar). The antioxidant activity of the compounds was determined using a Multiskan Go plate (96 wells) spectrophotometer (Thermo Fisher Sci., USA). The MTT test was carried out on a Zenyth200rt plate reader (Anthos).

Synthesis of 2,2'-[*(di-tert*-butylstannylene)bis(thio)]bis(benzoxazole) ¹¹⁹Bu₂Sn(Mbzo)₂ (I). Solid

potassium hydroxide (34 mg, 0.6 mmol) was added at room temperature with continuous stirring to a solution containing bis(*tert*-butyl)tin dichloride (91 mg, 0.3 mmol) and 2-mercaptopbenzoxazole (91 mg, 0.6 mmol) in methanol (3 mL). The mixture was stirred at room temperature for 2 h, and the formed light beige-colored crystalline precipitate was filtered off, washed with water and petroleum ether, and dried in air. The yield of compound I was 105 mg (65%).

IR (KBr pellets; ν , cm⁻¹): 3310–3110 br, 2966–2847, 1617 w, 1504 w, 1472 w, 1441 s, 1361 s, 1224 s, 1120 s, 1084 s, 1002 s, 929 m, 737 s, 642 m, 606 m, 545 m. ¹H NMR (CDCl₃), δ , ppm: 1.53 (s, 18H, 2(C(CH₃)₃, ³J_{H-Sn} 116 Hz), 7.21–7.35 (m, 4H, 2Ar), 7.35–7.45 (m, 4H, 2Ar). ¹³C NMR (CDCl₃), δ , ppm: 29.67 (C(CH₃)₃), 30.28 (C(CH₃)₃), 109.77, 116.61, 118.95, 123.54, 124.38, 149.56, 159.19. ¹¹⁹Sn NMR (CDCl₃), δ , ppm: -72.1.

Crystals of compound I suitable for XRD were isolated after the slow evaporation of a solution of the product in CHCl₃ at room temperature for 2 days.

For C₂₂H₂₆N₂O₂S₂Sn

Anal. calcd., % C, 49.55 H, 4.91 N, 5.25 S, 12.03
Found, % C, 49.72 H, 5.08 N, 5.12 S, 11.69

Synthesis of 2,2'-[*(di-tert*-butylstannylene)bis(thio)]bis(benzothiazole) ¹¹⁹Bu₂Sn(Mbzt)₂ (II). Solid potassium hydroxide (34 mg, 0.6 mmol) was added at room temperature with continuous stirring to a solution containing bis(*tert*-butyl)tin dichloride (91 mg, 0.3 mmol) and 2-mercaptopbenzothiazole (100 mg, 0.6 mmol) in methanol (3 mL). The mixture was stirred for 2 h and left to stay for 24 h, and the formed white crystalline precipitate was filtered off, washed with water and petroleum ether, and dried in air. The yield of compound II was 106 mg (63%).

IR (KBr pellets; ν , cm⁻¹): 3063 w, 2846–2973 m, 1586 w, 1560 w, 14659 w, 1453 m, 1414 s, 1409 s, 1361 m, 1236 m, 1143 s, 1073 s, 1007 s, 745 s, 720 s, 674 m, 604 m. ¹H NMR (CDCl₃), δ , ppm: 1.51 (s, 18H, 2(C(CH₃)₃, ³J_{H-Sn} = 112 Hz), 7.29 (dd, 2H, Ar, ³J_{H-H} = 8 Hz, ³J_{H-H} = 8 Hz), 7.42 (dd, 2H, Ar, ³J_{H-H} = 8 Hz, ³J_{H-H} = 8 Hz), 7.72 (d, 2H, Ar, ³J_{H-H} = 8 Hz), 7.73 (d, 2H, Ar, ³J_{H-H} = 8 Hz). ¹³C NMR (CDCl₃), δ , ppm: 29.90 (C(CH₃)₃), 30.33 (C(CH₃)₃), 119.29, 120.84, 123.55, 125.67, 126.24, 137.53, 151.56. ¹¹⁹Sn NMR (CDCl₃), δ , ppm: -42.9.

For C₂₂H₂₆N₂S₄Sn

Anal. calcd., % C, 46.73 H, 4.63 N, 4.95 S, 22.68
Found, % C, 46.52 H, 4.38 N, 5.13 S, 22.24

Synthesis of 2,2'-(di-*tert*-butylstannylene)bis(thio)bis(benzimidazole) $\text{Bu}_2\text{Sn}(\text{Mbzim})_2$ (III). Solid potassium hydroxide (34 mg, 0.6 mmol) was added at room temperature with continuous stirring to a solution containing bis(*tert*-butyl)tin dichloride (91 mg, 0.3 mmol) and 2-mercaptopbenzimidazole (91 mg, 0.6 mmol) in methanol (3 mL). The mixture was stirred for 2 h and left to stay for 24 h. The solvent was distilled off in *vacuo*, and the formed white finely crystalline precipitate was filtered off, washed with water and petroleum ether, and dried in air. The yield of compound **III** was 143 mg (90%).

IR (KBr pellets; ν , cm^{-1}): 3045–3300 m, 2806–2963 m, 1509 m, 1469 m, 1433 s, 1409 m, 1360 m, 1159 s, 1159 m, 1042 s, 1009 w, 963 w, 807 w, 736 s, 704 m, 651 m, 601 m. ^1H NMR (CDCl_3), δ , ppm: 1.35 (s, 18H, 2($\text{C}(\text{CH}_3)_3$), $^3J_{\text{H-Sn}} = 112$ Hz), 7.00–7.13 (m, 4H, $\text{CH}(\text{Ar})$), 7.14–7.24 (m, 2H, $\text{CH}(\text{Ar})$), 7.25–7.38 (m, 2H, $\text{CH}(\text{Ar})$), 12.55 (br.s, 2H, 2NH). ^{13}C NMR (CDCl_3), δ , ppm: 29.76 ($\text{C}(\text{CH}_3)_3$), 30.20 ($\text{C}(\text{CH}_3)_3$), 109.93, 122.27, 122.47, 123.87, 128.66, 139.17, 165.43. ^{119}Sn NMR (CDCl_3), δ , ppm: –140.3.

Crystals of complex **III** suitable for XRD were isolated after the slow evaporation of a solution of the product in CHCl_3 at room temperature for 4 days.

For $\text{C}_{22}\text{H}_{28}\text{N}_4\text{S}_2\text{Sn}$

Anal. calcd., % C, 49.73 H, 5.31 N, 10.54 S, 12.07
Found, % C, 50.06 H, 5.47 N, 10.38 S, 11.83

Synthesis of 2,2'-(di-*tert*-butylstannylene)bis(thio)bis(3,5-di-*tert*-butyl-4-hydroxyphenyl) $\text{Bu}_2\text{Sn}(\text{SR})_2$ (IV). A 1 M solution of KOH (0.4 mL, 0.4 mmol) was added dropwise at room temperature with stirring to a solution containing bis(*tert*-butyl)tin dichloride (61 mg, 0.2 mmol) and 2,6-di-*tert*-butyl-4-mercaptopphenol (95 mg, 0.4 mmol) in ethanol (4 mL). The mixture was stirred for 1 h, the solvent was distilled off in *vacuo* to half a volume, and the formed colorless needle-like crystals were filtered off, washed with water, and dried in air. The yield of compound **IV** was 81 mg (57%).

IR (KBr pellets; ν , cm^{-1}): 3632 s $\nu(\text{OH})_{\text{free}}$, 2847–2952 s $\nu(\text{CH})$, 1463 m, 1421 s, 1361 m, 1310 m, 1231 s, 1155 s, 1120 m, 1011 m, 879 m, 714 s, 618 w, 549 w. ^1H NMR (DMSO-d_6), δ , ppm: 1.43 (s, 36 H, 4($\text{C}(\text{CH}_3)_3$), $^3J_{\text{H-Sn}} = 92$ Hz), 5.14 (s, 2H, 2OH), 7.59 (s, 4H, $2\text{C}_6\text{H}_2$). ^{13}C NMR (DMSO-d_6), δ , ppm: 29.84 ($\text{C}(\text{CH}_3)_3$), 30.02 ($\text{SnC}(\text{CH}_3)_3$), 34.03 ($\text{C}(\text{CH}_3)_3$), 40.31 ($\text{SnC}(\text{CH}_3)_3$), 120.33 (C1), 131.88 (C2), 136.10

(C3), 152.71 (C4). ^{119}Sn NMR (DMSO-d_6); δ , ppm: 59.38.

Crystals of thiolate **IV** suitable for XRD were isolated after the slow evaporation of a solution of the product in CHCl_3 at room temperature for 1 day.

For $\text{C}_{36}\text{H}_{60}\text{O}_2\text{S}_2\text{Sn}$

Anal. calcd., % C, 61.10 H, 8.55 S, 9.06
Found, % C, 61.37 H, 8.67 S, 8.79

XRD was carried out on a Bruker Quest D8 diffractometer equipped with a Photon-III detector (MoK_α radiation, ϕ and ω scan modes). Taking into account a strongly anisotropic shape of the crystals, an absorption correction was applied using a multiple scanning procedure implemented in SADABS (version 2016/2) [13]. The structures were solved by dual methods using the SHELXT program and refined for F_{hkl}^2 using the SHELXL-2018 program [14]. Positions of hydrogen atoms (except for the OH group) were calculated. The atoms were refined with individual anisotropic or isotropic (hydrogen atoms) shift parameters. Quantum-chemical calculation was performed using the Gaussian09 software [15] by the PBE0 [16] functional and def-2-TZVP basis set. The experimentally obtained geometry in the crystal for **II** was used in the calculation, except for the hydrogen atoms for which the C–H distances were normalized to the ideal neutronographic values. Dispersion interactions were taken into account by applying an empirical dispersion correction [17]. A topological analysis of the electron density distribution function $\rho(r)$ was performed using the AIMAll program [18]. All expected critical points were localized during the calculation, and the obtained set of critical points satisfied the Poincaré–Hopf equation.

The main crystallographic characteristics and XRD experimental parameters for the structures of compounds **I**, **II**, and **IV** are listed in Table 1. Selected bond lengths and angles are given in Table 2.

The full set of XRD parameters was deposited with the Cambridge Crystallographic Data Centre (CIF files CCDC nos. 2251495 (**I**), 2251493 (**II**), 2251494 and (**IV**)), deposit@ccdc.cam.ac.uk; <http://www.ccdc.cam.ac.uk>).

Inhibition of lipoxygenase enzyme. The activity of lipoxygenase enzyme (LOX 1-B) was determined by spectrophotometry measuring the content of the products of linoleic acid oxidation: the corresponding isomeric hydroperoxides at $\lambda_{\text{max}} = 234$ nm [11, 19].

The degree of inhibition of lipoxygenase (I , %) was determined by the equation

$$I = v_o(\text{solution of substance})/v_o(\text{DMSO}) \times 100\%,$$

where v_o and v_o (DMSO) is the rate of enzymatic oxidation of linoleic acid in the presence of the tested

compound (1 mM, borate buffer, pH 9.0) and in the control without compound, respectively.

Table 1. Crystallographic characteristics and experimental details for compounds **I**, **II**, and **IV**

Parameter	Value		
	I	II	IV
Empirical formula	C ₂₂ H ₂₆ N ₂ O ₂ S ₂ Sn	C ₂₂ H ₂₆ N ₂ S ₄ Sn	C ₃₆ H ₆₀ O ₂ S ₂ Sn
<i>FW</i>	565.38	533.26	707.64
<i>T</i> , K	100	110	110
Crystal system		Monoclinic	
Space group	<i>C</i> 2/ <i>c</i>	<i>P</i> 2 ₁ / <i>c</i>	<i>C</i> 2/ <i>c</i>
<i>Z</i> (<i>Z'</i>)	4(0.5)	4	4(0.5)
<i>a</i> , Å	22.577(4)	11.9615(5)	17.630(2)
<i>b</i> , Å	6.9723(13)	14.0895(7)	18.040(3)
<i>c</i> , Å	15.729(3)	14.2586(8)	12.4200(17)
β, deg	113.374(7)	94.821(2)	95.796(5)
<i>V</i> , Å ³	2272.9(7)	2394.5(2)	3929.9(10)
ρ _{calc} , g cm ⁻³	1.558	1.568	1.196
μ, cm ⁻¹	13.28	14.28	7.83
<i>F</i> (000)	1080	1144	1496
2θ _{max} , deg	58	62	60
Number of measured reflections	10821	26033	19022
Number of independent reflections	3019	7347	5212
Number of reflections with <i>I</i> > 2σ(<i>I</i>)	2332	6158	4612
Number of refined parameters	135	268	196
<i>R</i> ₁	0.0429	0.0358	0.0390
<i>wR</i> ₂	0.0934	0.0829	0.0950
GOOF	1.008	1.025	1.051
Residual electron density (max/min), e Å ⁻³	1.518/-0.709	0.744/-0.459	1.192/-0.357

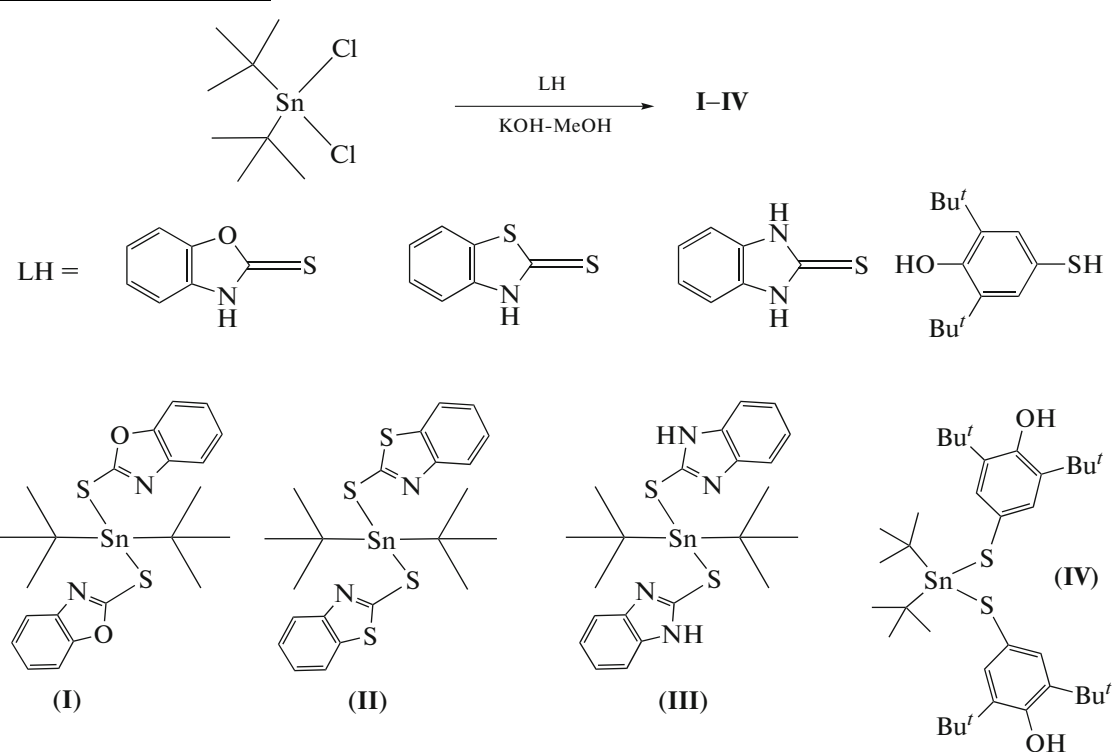
Table 2. Selected bond lengths (Å) and angles (deg) for compounds **I**, **II**, and **IV**

Complexes	I	II	IV
Bond lengths, Å			
Sn—S	2.5214(10)	2.5111(6), 2.5160(6)	2.4292(6)
Sn—C	2.210(4)	2.197(2), 2.202(2)	2.179(2)
Sn...N	2.888(4)	2.792(1), 2.911(1)	
Bond angles, deg			
SSnS	84.00(4)	83.15(2)	110.11(3)
CSnC	134.84(19)	133.15(9)	118.51(14)
SSnN	59.12(7)	59.83(4)	
NSnN	158.32(19)	159.53(8)	

MTT test [20] was carried out by a modified procedure [2]. Experiments with the tested compounds were conducted in three repetitions on a Zenyth 2000rt plate reader at a wavelength of 570 nm. The results of the test were presented as a plot of the dependence of % survived cells on the concentration of the studied substances. Cisplatin served as the standard.

RESULTS AND DISCUSSION

Tin(IV) bis(thiolates) were synthesized by the reactions of di-*tert*-butyltin dichloride with heterocyclic thioamides or 2,6-di-*tert*-butyl-4-hydroxyphenylmercaptophenol (Scheme 1).



Scheme 1.

The compositions and purity of the organotin complexes were confirmed by ^1H and ^{13}C NMR spectroscopy, IR spectroscopy, and elemental analysis. The yields of the compounds were 57–90%. Remarkably, the IR spectrum of complex **IV** exhibits a narrow absorption band at 3632 cm^{-1} corresponding to stretching vibrations of the O–H bond of the sterically hindered unassociated phenol group, and stretching vibrations of the C–H bond are observed in a range of ~ 2847 – 2952 cm^{-1} .

In the ^1H NMR spectra of compounds **I**–**IV**, the protons of the *tert*-butyl groups at the tin atom appear as an equivalent singlet in a range of 1.35–1.53 ppm depending on the ligand nature, and the H–Sn spin–spin interaction of the Sn–C(CH₃)₃ fragment with the constants $^3J_{\text{H–Sn}} = 92$ – 116 Hz is observed. For the group of complexes **I** and **II** with benzoxazole and benzothiazole as ligands, the $^3J_{\text{H–Sn}}$ constants remain nearly unchanged compared to $^3J_{\text{H–Sn}} = 112\text{ Hz}$ for the starting $^3\text{Bu}_2\text{SnCl}_2$ in CDCl₃. When chloride in compound **IV** is substituted by the mercaptophenol frag-

ment, $^3J_{\text{H–Sn}}$ decreases substantially from 124 to 92 Hz compared to that of $^3\text{Bu}_2\text{SnCl}_2$ in CDCl₃. Complex **III** based on benzimidazole is poorly soluble in chloroform and, hence, its NMR spectra were recorded in DMSO. The constant $^3J_{\text{H–Sn}} = 124\text{ Hz}$ of $^3\text{Bu}_2\text{SnCl}_2$ in DMSO-d₆ also decreased upon the introduction of benzimidazole in complex **III** to 92 Hz, which indicates the electron density redistribution.

The ^{119}Sn NMR spectra of complexes **I**–**IV** indicate the influence of the ligand nature on the chemical shift of the tin core, which varies from -140 (**III**) to $+59\text{ ppm}$ (**IV**).

The XRD studies of complexes **I**, **II**, and **IV** showed that two corresponding ligands and two *tert*-butyl substituents entered the coordination sphere of the tin atom in all complexes (Figs. 1–3). In two complexes (**I** and **IV**), the tin atom lies on axis 2, whereas in complex **II** all atoms occupy the general position. In spite of the same stoichiometric composition and similar (as a whole) local symmetry, the coordination environment of the tin atom differs substantially in complexes **I**, **II**, and **IV**. For instance, the coordina-

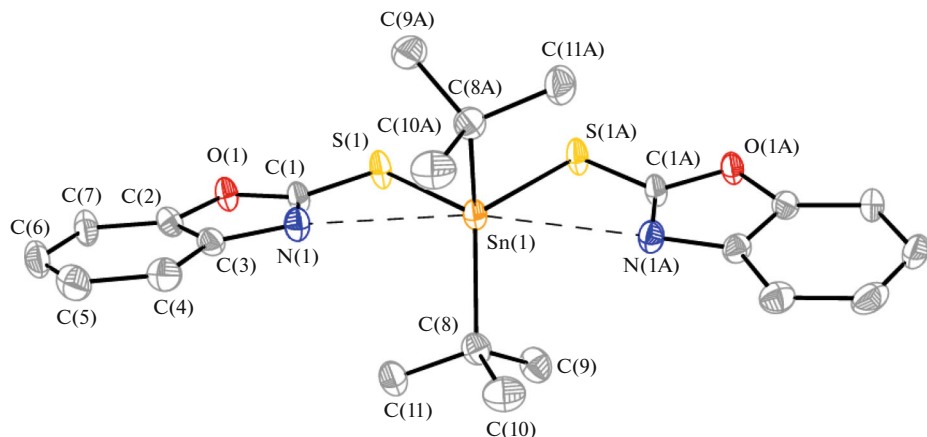


Fig. 1. General view of complex I in representation of atoms by atomic shift ellipsoids ($p = 50\%$).

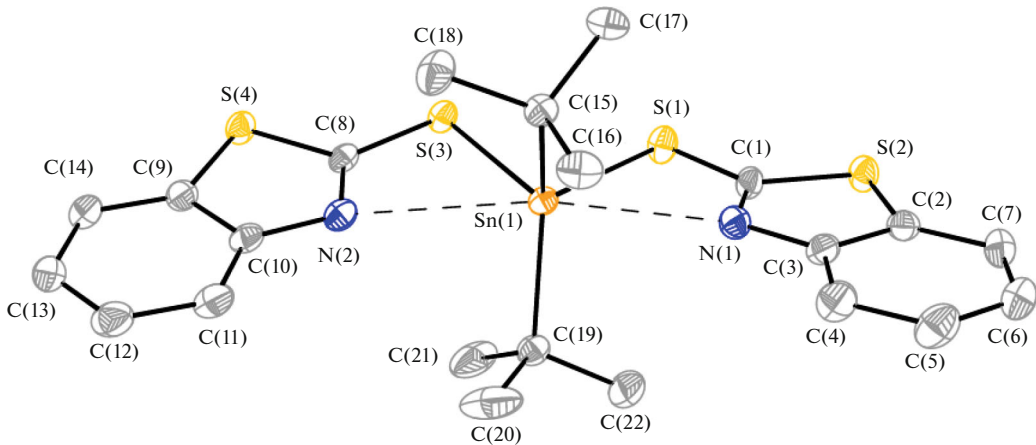


Fig. 2. General view of complex II in representation of atoms by atomic shift ellipsoids ($p = 50\%$).

tion polyhedron in complex **IV** can undoubtedly be described as an insignificantly distorted tetrahedron (coordination number 4) in which the CSnC and SSnS angles are $118.51(14)^\circ$ and $110.11(3)^\circ$ (Fig. 3). On the contrary, an additional coordination with the nitrogen atom in the heterocycles is observed in complexes **I** and **II** along with the expected $\text{Sn}-\text{C}$ and $\text{Sn}-\text{S}$ bonds (Figs. 1, 2; Table 2). The existence of $\text{Sn} \dots \text{N}$ interactions is indicated by the distance $(2.792(1)-2.911(1) \text{ \AA})$, which can be a consequence of the forced shortening of the contact, and also a substantial increase in the CSnC bond angle to $133.15(9)^\circ-134.84(19)^\circ$ in complexes **I** and **II** compared to compound **IV**. In spite of the assumed increase in the coordination number from 4 to 6, the $\text{Sn}-\text{C}$ bonds in complexes **I** and **II** elongate by at most 0.02 \AA compared to those in complex **IV**.

A topological analysis of the electron density distribution function was used in the framework of R. Bader's theory "Atoms in Molecule" (AM) [21] with the purpose of an independent estimation of the

energy of interactions in the first coordination sphere of tin. According to the AM theory, the existence of a binding interaction means the presence of the critical point (CP) $(3, -1)$ of the electron density function and, which is similarly, binding route: the line of the maximum gradient of the electron density connecting two atomic nuclei. In the case of the CP $(3, -1)$ for this interaction, its energy (E_{cont}) can semiquantitatively be estimated from the local density of the potential energy $v(r)$ at the CP: Espinosa–Molins–Lecomte (CEML) relationship [22]. The CEML relationship was independently substantiated physically [23] and was shown to give correct estimates for both hydrogen bonds and coordination interactions, such as $\text{Gd}-\text{X}$ ($\text{X} = \text{O}, \text{N}, \text{Cl}$) [24], $\text{Au}-\text{P}$ [25], $\text{Pd}-\text{C}$ [26], and $\text{Zn}-\text{N}$ [27].

Based on the experimental geometry, we calculated the electron density function for complex **I** and performed the topological analysis. The search for the CP $(3, -1)$ showed that both the considered $\text{Sn} \dots \text{N}$ interactions and $\text{Sn}-\text{S}$ and $\text{Sn}-\text{C}$ interactions correspond

to attractive interactions: the critical points (3, -1) were localized for them. However, the character of interactions somewhat differs. The interactions with the sulfur atom and *tert*-butyl group correspond to interactions of an intermediate type, which is indicated by the positive electron density Laplacian ($\nabla^2\rho(r)$) at the negative density of the electron energy ($H_e(r)$). As can be seen from Table 3, the Sn...N interaction is an interaction of the type of closed shells with allowance for positive $H_e(r)$ and, therefore, is characterized by a substantially lower covalent contribution. The estimation of E_{cont} for these interactions shows that Sn...N (8.7 kcal/mol) is almost an order of magnitude weaker than the interactions with the sulfur and carbon atoms and is lower than E_{cont} for strong hydrogen bonds [28]. Starting from this, we can assume that, in the case of a specific solvation in the solution, the coordination environment of tin can change due to competitive interactions solvent...nitrogen atom. This conclusion is consistent in part with the described data for similar tin(IV) complexes [29]. An analysis of intermolecular interactions showed that the interatomic distances correspond to usual van der Waals interactions in all complexes. The main contribution is made by contacts of the H...H type because of interactions between the *tert*-butyl substituents.

The ability of complexes **I**–**IV** to inhibit lipoxygenase enzyme was studied in the oxidation of linoleic acid under the action of lipoxygenase LOX 1-B. An importance of lipoxygenase as a pharmacological target is due to both its involvement in the synthesis of leucotrienes and, as a consequence, the ability to promote inflammatory processes and the generation from arachidonic acid of 5-hydroxyeicosatetraenoic acid (5-HETE), which further becomes a factor of survival of prostate cancer cells [30, 31]. Therefore, there were many attempts to search for a selective inhibitor of lipoxygenase [32]. The enzymatic oxidation of linoleic acid to the corresponding hydroperoxides was detected by spectrophotometry from an increase in the absorbance of the solution at $\lambda = 234$ nm. The generation rate of linoleic acid hydroperoxides in the presence of 1 mM tested compounds was compared with the control and expressed in % inhibition. The degree

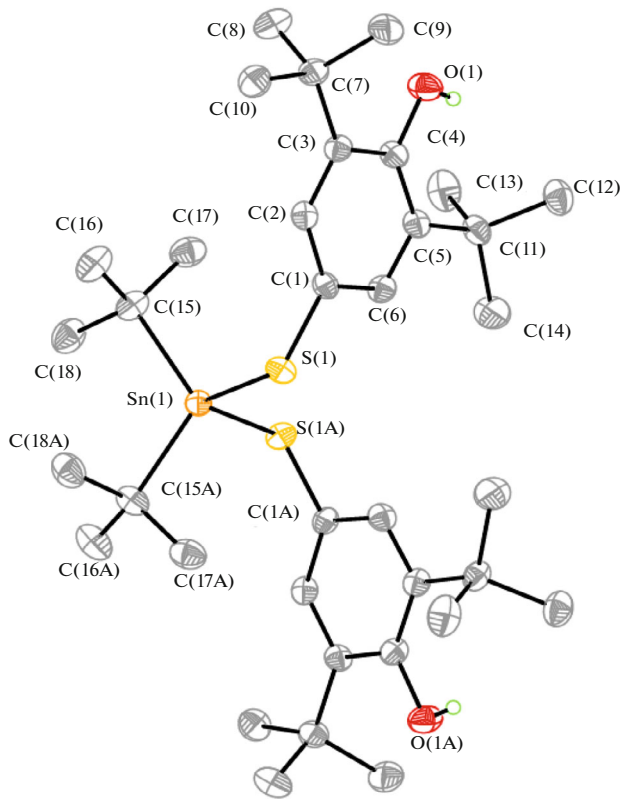


Fig. 3. General view of complex **IV** in representation of atoms by atomic shift ellipsoids ($p = 50\%$).

of inhibition of LOX 1-B enzyme by compounds **I**–**IV** is given below.

Compound	I	II	III	IV
<i>I</i> , %	52.6 ± 4.1	30.5 ± 2.8	7.0 ± 1.1	15.4 ± 1.9

Complexes **I**–**IV** demonstrate a moderate inhibitory activity toward LOX 1-B. Benzoxazole derivative **I** is the hit compound, whereas 2-mercaptopbenzimidazole complex **III** manifested the lowest activity.

The screening results of the anticancer activity of tin complexes **I**–**IV** by the MTT method on the PC3, MCF-7, HCT116, and A549 cell lines and normal WI38 cells are given in Table 4.

Table 3. Main topological parameters* at the CP (3, -1) for the bonds involving the tin atom in an isolated molecule of compound **I** according to the PBE0/def2TZVP calculation data

Bond	$\rho(r)$, e \AA^{-3}	$\nabla^2\rho(r)$, e \AA^{-5}	$H_e(r)$, au	$v(r)$, au	E_{cont} , kcal/mol
Sn–S	0.473	2.00	-0.0214	-0.0636	-42.8
Sn–N	0.130	1.25	0.001	-0.0129	-8.7
Sn–C	0.669	1.10	-0.0394	-0.0903	-60.8

* $\rho(r)$ is the electron density function, $\nabla^2\rho(r)$ is the electron density Laplacian, $H_e(r)$ is the local density of the electron energy, and $v(r)$ is the local density of the potential energy.

Table 4. Values of IC_{50} for compounds **I**–**IV** and cisplatin on the cell lines*

Compound	IC_{50} , μM				
	PC3	MCF7	HCT116	A549	WI38
I	0.2 \pm 0.05	0.4 \pm 0.1	2.1 \pm 0.2	2.9 \pm 0.7	0.7 \pm 0.1
II	0.5 \pm 0.01	1.2 \pm 0.5	2.1 \pm 0.3	2.9 \pm 0.8	0.8 \pm 0.1
III	0.020 \pm 0.005	0.7 \pm 0.05	2.5 \pm 0.2	3.6 \pm 1.0	0.30 \pm 0.05
IV	>100	12.1 \pm 2.6	51.3 \pm 5	79 \pm 11	32 \pm 5
Cisplatin	2.2 \pm 0.8	15.5 \pm 3	7.1 \pm 1.5	10.4 \pm 1.5	5.5 \pm 0.3

* PC3 (prostate cancer), MCF-7 (breast adenocarcinoma), HCT-116 (colon cancer), A549 (lung adenocarcinoma), and WI38 (normal fibroblast cells from the lung tissue).

Thus, new organotin complexes with the ligands based on heterocyclic thioamides and 2,6-di-*tert*-butyl-4-mercaptophenol were synthesized. The molecular structures of complexes **I**, **II**, and **IV** containing 2-mercaptopbenzoxazole, 2-mercaptopbenzothiazole, and 2,6-di-*tert*-butyl-4-mercaptophenol were determined by XRD. The ability of the compounds to inhibit the LOX-1B lipoxygenase enzyme as one of the targets for anticancer drugs was studied. Compounds **I** and **II** were found to manifest a high inhibitory activity. The antiproliferative properties of the compounds were studied by the MTT test on both the cancer and healthy cells. The values of IC_{50} for the synthesized compounds against the HCT-116, MCF-7, A-549, and WI38 cells were revealed to depend substantially on the ligand nature. Benzimidazole complex **III** has the highest antiproliferative activity: its activity is by two orders of magnitude higher than that of cisplatin on the PC3 prostate cancer line. The introduction of the antioxidant 2,6-di-*tert*-butylphenol fragment into complex **IV** decreases the cytotoxicity by 1.5–50 times depending on the type of the cell line.

The results demonstrate a selectivity of the action of the complexes toward prostate cancer cells, which provides new prospects when searching for new anticancer drugs for the therapy of prostate cancer.

ACKNOWLEDGMENTS

XRD studies were carried out on the equipment of the Center for Collective Use at the Department of Chemistry of the Moscow State University purchased in the framework of the Moscow University development program.

FUNDING

This work was supported by the Russian Science Foundation, project no. 22-23-00295.

CONFLICT OF INTEREST

The authors of this work declare that they have no conflicts of interest.

REFERENCES

1. Milaeva, E.R., Dodokhova, M.A., Shpakovsky, D.B., et al., *J. Biomed.*, 2021, vol. 17, p. 88. <https://doi.org/10.33647/2074-5982-17-2-88-99>
2. Antonenko, T.A., Gracheva, Yu.A., Shpakovsky, D.B., et al., *Int. J. Mol. Sci.*, 2023, vol. 24, p. 2024.
3. Nikitin, E., Mironova, E., Shpakovsky, D., et al., *Molecules*, 2022, vol. 27, p. 8359.
4. Milaeva, E.R., Shpakovsky, D.B., Gracheva, Yu.A., et al., *Pure Appl. Chem.*, 2020, vol. 92, p. 1201.
5. Shpakovsky, D.B., Banti, C.N., Mukhatova, E.M., et al., *Dalton Trans.*, 2014, vol. 43, no. 18, p. 6880.
6. Milaeva, E.R., Shpakovsky, D.B., Gracheva, Yu.A., et al., *J. Organomet. Chem.*, 2015, vol. 782, p. 96.
7. Banti, C.N., Hadjikakou, S.K., Sismanoglu, T., et al., *J. Inorg. Biochem.*, 2019, vol. 194, p. 114.
8. Chaurasiya, A., Sahu, C., Wahan, S.K., et al., *J. Mol. Struct.*, 2023, vol. 1280, p. 134967.
9. Bandaru, P.K., Rao, N.S., Radhika, G., et al., *Chem. Data Coll.*, 2023, vol. 44, p. 100994.
10. Orafaiea, A., Mousavianb, M., Orafaic, H., et al., *Prostaglandins and Other Lipid Mediators*, 2020, vol. 148, p. 106411.
11. Xanthopoulou, M.N., Hadjikakou, S.K., Hadjiliadis, N., et al., *Eur. J. Med. Chem.*, 2008, vol. 43, p. 327.
12. Muller, E., Stegman, H.B., and Scheffler, K., *Liebigs Ann. Chem.*, 1961, vol. 645, p. 79.
13. Krause, L., Herbst-Irmer, R., Sheldrick, G.M., et al., *J. Appl. Crystallogr.*, 2015, vol. 48, p. 3.
14. Sheldrick, G.M., *Acta Crystallogr. Sect. C: Struct. Chem.*, 2015, vol. 71, p. 3.
15. Frisch, M.J., Trucks, G.W., Schlegel, H.B., et al., *Wallingford (CT): Gaussian 09, Revision D.01*, Gaussian, Inc., 2016.
16. Perdew, J., Ernzerhof, M., and Burke, K., *J. Chem. Phys.*, 1996, vol. 105, p. 9982.
17. Grimme, S., Antony, J., Ehrlich, S., et al., *J. Chem. Phys.*, 2010, vol. 132, p. 154104.
18. Keith, T., *AIMAll (version 16.08.17)*, Overland Park (KS): TK Gristmill Software, 2016. <https://aim.tkgristmill.com>.
19. Mikhalev, O.V., Shpakovsky, D.B., Gracheva, Yu.A., et al., *Russ. Chem. Bull.*, 2018, vol. 67, no. 4, p. 712. <https://doi.org/10.1007/s11172-018-2127-2>

20. Niks, M. and Otto, M., *J. Immunol. Methods*, 1990, vol. 130, no. 1, p. 149.
21. Matta, C.F. and Boyd, R.J., *The Quantum Theory of Atoms in Molecules: From Solid State to DNA and Drug Design*, Wiley-VCH, 2007.
22. Espinosa, E., Molins, E., and Lecomte, C., *Chem. Phys. Lett.*, 1998, vol. 285, p. 170.
23. Ananyev, I.V., Karnoukhova, V.A., Dmitrienko, A.O., and Lyssenko, K.A., *J. Phys. Chem.*, 2017, vol. 121, p. 4517.
24. Puntus, L.N., Lyssenko, K.A., Antipin, M.Yu., et al., *Inorg. Chem.*, 2008, vol. 47, p. 11095.
25. Borissova, A.O., Korlyukov, A.A., Antipin, M.Y., et al., *J. Phys. Chem.*, 2008, vol. 112, p. 11519.
26. Vatsadze, S.Z., Medved'ko, A.V., Zyk, N.V., et al., *Organometallics*, 2009, vol. 28, p. 1027.
27. Abdulaeva, I.A., Birin, K.P., Sinelshchikova, A.A., et al., *CrystEngComm*, 2019, vol. 21, p. 1488.
28. Lyssenko, K.A., *Mendeleev Commun.*, 2012, vol. 22, no. 1, p. 1.
29. Xanthopoulou, M.N., Hadjikakou, S.K., Hadjiliadis, N., et al., *Inorg. Chem.*, 2007, vol. 46, p. 1187.
30. Ghosh, J. and Myers, C.E., *Biochem. Biophys. Res. Commun.*, 1997, vol. 235, no. 2, p. 418.
31. Ghosh, J. and Myers, C.E., *PNAS*, 1998, vol. 95, no. 22, p. 13182.
32. Werz, O. and Steinhilber, D., *Pharmacol. Ther.*, 2006, vol. 112, no. 3, p. 701.

Translated by E. Yablonskaya